Magazine of Concrete Research
Volume 68 Issue 1
Punching shear strength of RC flat slabs at interior connections to columns
Bompa and Oneț

Magazine of Concrete Research, 2016, **68**(1), 24–42
http://dx.doi.org/10.1680/macr.14.00402
Paper 1400402
Received 26/11/2014; revised 26/03/2015; accepted 10/04/2015
Published online ahead of print 30/05/2015

ice Institution of Civil Engineers
publishing

Punching shear strength of RC flat slabs at interior connections to columns

Dan V. Bompa
Post-doctoral Research Associate, Imperial College London, London, UK

Traian Oneț
Professor, Technical University of Cluj-Napoca, Cluj-Napoca, Romania

A method to evaluate the punching shear strength of reinforced concrete (RC) flat slabs without shear reinforcement at the connection to interior columns is proposed. The method is based on the assumption that the punching shear strength is controlled by the inclination of a unique punching shear crack that produces a conical failure surface. The inclination angle of the crack is variable. It follows that the location of the critical section is not established in advance, but changes with crack angle. Its location depends on the reinforcement ratio, material strengths and effective depth. According to the proposed method, the punching shear strength is a function of the inclination angle of the governing crack that controls the amount of shear carried by the compression zone and the flexural reinforcement crossing the potential punching cone by accounting for its slenderness and concrete size effect. The method describes the behaviour observed in tests and numerical and analytical investigations. The novel premise that the punching shear strength of flat slabs at connections to interior columns is controlled by the inclination of the failure surface shows remarkable agreement with the results of 209 tests on isolated specimens reported in the literature. This paper also assesses the adequacy of strength predictions obtained using the proposed method and the methods adopted in the codified provisions.

Notation

A_{pc}	area of crack interface (punching cone)
b_0	control perimeter
b_c	column dimension
d	effective depth
d_i	damage parameter
d_g	aggregate size
E_c	concrete modulus of elasticity
E_s	steel modulus of elasticity
f_c	concrete compressive strength on cylinder tests
f_{ct}	concrete tensile strength
f_v	shear strength of plain concrete
f_y	yield strength of flexural reinforcement
G_f	fracture energy ($G_f = 73(f_c)^{0·18}$)
h_s	slab thickness
K_c	shape of deviatoric plane
l_0	length of punching crack pattern at top face of slab at centroid of flexural reinforcement predicted by Equation 9
l_{ch}	fractal parameter of concrete ($l_{ch} = G_f E_c/(2f_{ct})$)
l_s	span
p, q	stress invariants, load
m	bending moments
r_0	radius of punching crack at top face of slab
r_s	slab radius
V	punching shear strength
V_{flex}	flexural strength
β	internal friction angle
ε	strain
ϵ	eccentricity of plastic surface
θ	crack inclination
λ	slenderness of punching cone
ξ	size effect
ρ	flexural reinforcement ratio
σ	stress
τ	tangential stress
ϕ	dilation angle of material
ψ	rotation
ω	mechanical reinforcement ratio

Introduction

Situations in which the use of flat-slab structural systems has proved to be effective are countless. The solution has attracted much attention due to its simple and advantageous construction process. The design of such systems is typically governed by localised effects such as large midspan deflections in service or punching shear at ultimate. Uncertainties mainly exist regarding the behaviour of the connection region between the slab and the column. At interior columns, investigated here as isolated slab regions, the behaviour is potentially governed by punching shear even under sole gravity loading.

In three-dimensional (3D) reinforced concrete (RC) elements such as suspended slabs or footings, the behaviour in the connection region to the column is characterised by the

development of flexural cracks at incipient loading stages (Figures 1(a) and 2(c)). At ultimate state they may govern, leading to a potential yielding of the longitudinal reinforcement (typical case for low amounts, see Figure 3(c) (Hallgren, 1996)). When flexural failure is not governing, but stresses in reinforcement bars are close to the yield stresses, flexural cracks propagate into shear cracks, leading to a failure mode defined as flexural punching (fib, 2001).

In the case of high reinforcement ratios, a slab will show stiffer behaviour, characterised by low stresses in the reinforcement and high stresses in the inclined concrete compression stress field that develops in the vicinity of the column (Figure 2(c)). A brittle failure, called punching shear, occurs when the inclined compression zone is unable to sustain any load increment (e.g. test HSC0 in Figure 3(a) (Hallgren, 1996)). Punching shear failure is described as the development of a diagonal crack of variable inclination starting from the face of the column (in the compression side of the slab) and ending at the tension face of the slab, resulting in the dislocation of a conical body from the concrete slab (Regan, 1986).

In concrete members, shear is typically carried through cracked interfaces by frictional resistance of the aggregates against crack slip and growth (Walraven and Reinhardt, 1981), shearing of the dowel bar (Dei Poli *et al.*, 1987, 1992; Ince *et al.*, 2007; Paulay and Loeber, 1974; Taylor, 1970),

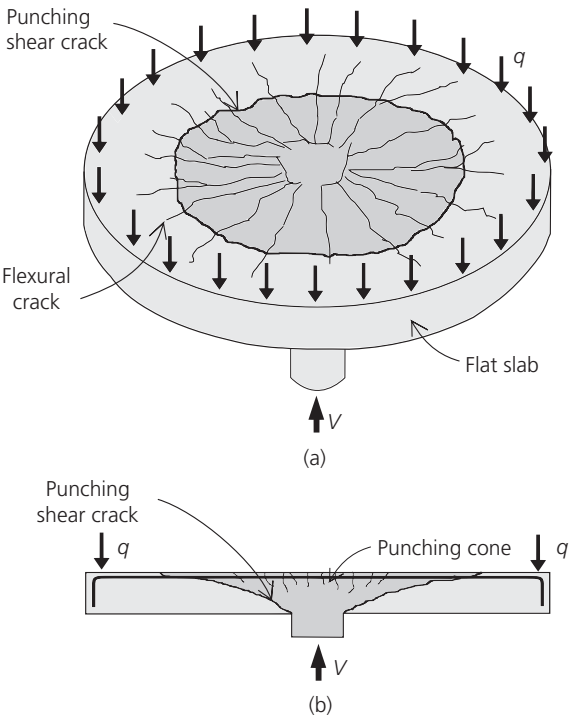

Figure 1. Isolated interior flat-slab–column region and typical punching shear failure surface: (a) isometric view; (b) section

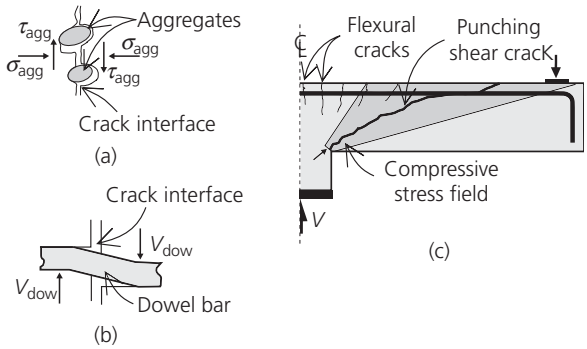

Figure 2. (a) Aggregate interlock. (b) Dowel action. (c) Compression field

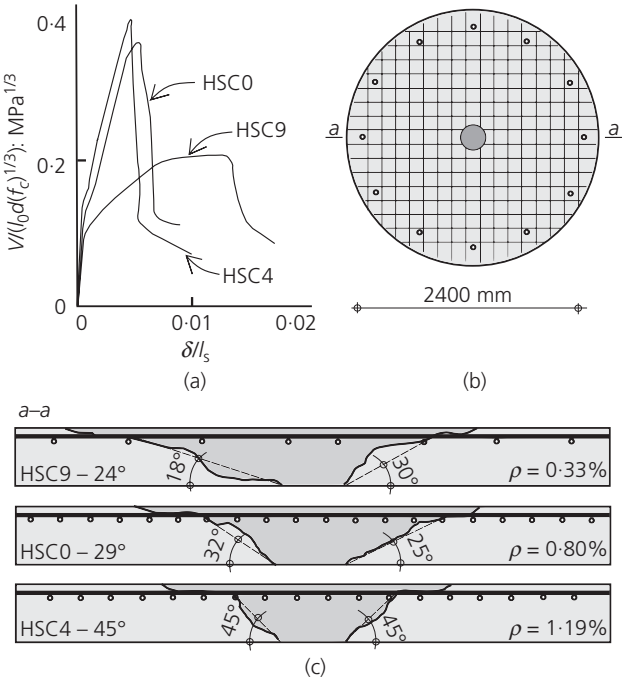

Figure 3. Tests (HSC0, HSC4 and HSC9) carried out by Hallgren (1996): (a) structural response; (b) in-plane geometrical configuration; (c) sectional views as a result of saw cuts

transfer through the concrete compression zone (Chana, 1987) and transfer of residual stresses through the crack tip (see Figures 2(a) and 2(b)). The inclination of the punching shear crack is governed by the stress distribution in the connection region. Its punching shear strength is governed by the amount of shear carried through the cracked interface. The inclination of the crack and the amount of shear carried through it are dependent on the geometry of the member (depth, slenderness, column dimension to slab thickness) and the characteristics of the structural parameters (material strengths, aggregate distribution and dimension, reinforcement layout etc.).

The magnitude of shear transferred by aggregate interlock is dependent on the inclination of the cracked interface: the flatter the inclination angle, the higher the interlocking surface and, consequently, in the case of slabs, the higher the amount of shear transferred by this action. On the other hand, the length of the intersection line between the punching cone and the reinforcement plane is also controlled by the inclination of the governing punching shear crack. As the crack inclination angle reduces, the number of bars subjected to dowel action increases. Regan and Braestrup (1985) reported that 34% of the ultimate punching shear strength is attributed to this mechanism. Hence, the inclination of the governing punching shear crack is a key parameter that controls the punching shear strength of slabs.

Although intense research has been done in recent decades in this field (e.g. Bazant and Cao, 1987; Broms, 1990; Elstner and Hognestad, 1956; Hallgren, 1996; Hegger *et al.*, 2009; Kinnunen and Nylander, 1960; Muttoni, 2008; Regan, 1986), punching shear is still a polemic topic and methods to improve the phenomenological understanding and advancement in the state of the art are needed. This paper proposes a novel method to assess the punching shear strength of flat slabs without transverse reinforcement at the connection to interior columns. The method is based on the assumption that the key parameter that controls the punching shear strength is the inclination of the punching shear crack, which increases linearly with reinforcement ratio and effective depth. The location of the critical section varies with slab geometry and material characteristics. In the case of steep crack angles, the critical section lies closer to the column whereas, for flat crack angles, the critical section is found further from the column.

The component-based method proposed here accounts for the contribution of the following variables: concrete compression zone, interlocking of the aggregates, the dowel action of the reinforcement bars, the shape and slenderness of the punching cone and concrete-specific size effect. The magnitude of each variable is controlled by the inclination of the punching shear crack. The method is based on information obtained in tests (Bompa and Oneț, 2011; Gosav *et al.*, 2013) and numerical parametric and analytical studies. Compared with existing design guidelines it offers better control since it accounts for a higher variety of structural parameters. The method is applicable to the evaluation of the punching shear strength of flat slabs without shear reinforcement connected to interior columns with circular or rectangular cross-sections. It shows remarkable agreement with the results of a series of 209 tests on isolated specimens reported in the literature (suspended slabs and footings) and can be successfully applied to the design of continuous flat slabs since the beneficial effect of compressive membrane action, disregarded here, may increase the punching shear strength at ultimate state. The paper also assesses the adequacy of the method in comparison with the predictions of current codified approaches.

Parameters governing punching shear strength

Figure 4(a) plots the relationship between the normalised punching shear strength and the concrete strength of specimens from the available database ($V/l_0 d(f_c)^{1/3}$, where V is the reported punching shear strength in tests). Hallgren (1996) reported that an increase in concrete strength (f_c) from 25 MPa to 90 MPa for a flexural reinforcement ratio of 0·8% brought a significant increase (50–60%) in punching shear strength whereas, for a low reinforcement ratio (ρ = 0·3%) the corresponding increase was 20% (Figure 3). The use of high-strength concrete with a low reinforcement ratio resulted in bending controlled failure (flexural punching), whereas the use of normal-strength concrete for the same ρ resulted in brittle punching without reaching the flexural strength (Hallgren, 1996). Inacio *et al.* (2013) showed that an increase in concrete strength (from 35 MPa to 125 MPa) resulted in the development of higher brittleness.

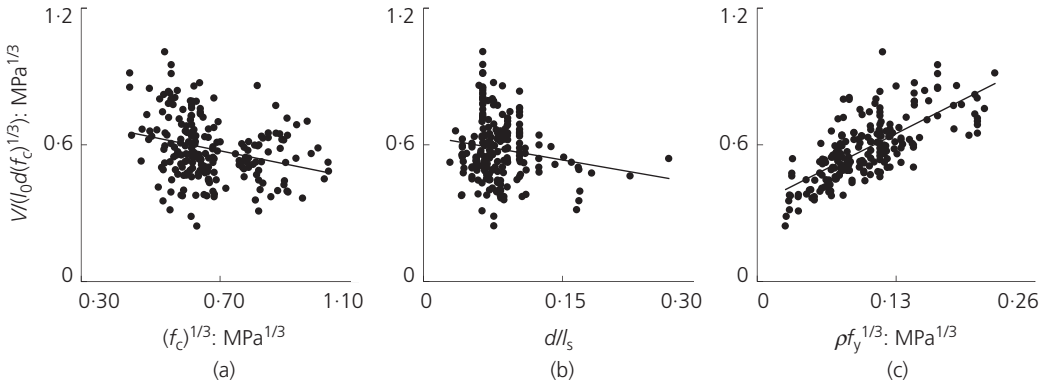

Figure 4. Analytical study on key parameters on reported test database for the influence of (a) concrete strength, (b) slab slenderness and (c) reinforcement ratio

One of the key parameters in increasing the punching shear strength is the thickness of the slab. The modification of thickness from 200 mm to 260 mm for a high reinforcement ratio ($\rho = 1{\cdot}25\%$), accounting for low concrete strength ($f_c < 20$ MPa) and variable slenderness, resulted in a 28% decrease in nominal strength (Gosav *et al.*, 2013). Slenderness was likewise reported to be key parameter in the behaviour of flat slabs (Moe, 1961). According to the test database, a slender specimen has a lower nominal punching strength, whereas a more robust one shows an increase in nominal punching strength (Figure 4(b)).

Maintaining a constant aspect ratio, Guandalini *et al.* (2009) tested a series of full-scale specimens with a low amount of bending reinforcement ($\rho = 0{\cdot}33\%$) and varying thickness of 250–500 mm. The nominal capacity of the 500 mm thick specimen was 17% smaller than that of the 250 mm thick specimen. It can be said that an increase in thickness has a greater influence for specimens with moderate and high flexural reinforcement ratios. In addition, an increase in thickness has a comparatively lower effect on the nominal punching capacity for thin slabs ($h_s < 200$ mm), but a considerable effect for thick ones ($h_s > 200$ mm). The size effect, characteristic for brittle materials such as concrete, was previously addressed for flat slabs by Bazant and Cao (1987), Broms (1990) and Menetrey (2002).

Figure 4(c) shows the relationship between the reinforcement ratio and ultimate strength on a series of tests gathered from the database (Table 1). For low reinforcement ratios, bending-controlled behaviour develops, leading to potential flexural failures. The behaviour of slabs with low reinforcement is characterised by flexibility, higher deflections and flatter governing punching shear cracks. On the other hand, slabs with high reinforcement ratios develop a stiff behaviour characterised by small deflections and steep diagonal cracks (Figures 3(a) and 3(c)). On the same topic, Regan (1986) reported that, in the case of slabs when the failure surface crosses the reinforcement, the nominal stress is proportional to the cube root of the ratio of reinforcement, which is faithfully captured in Figure 4(c).

Numerical investigation

This section describes numerical investigations carried out using the finite-element package Abaqus 6.10 (DSS, 2010) to obtain insight into the force transfer paths within a concrete body. The objective of the investigation was to see the effect of a change in slab thickness on the angle of the compression stress field. The concrete damaged plasticity model (CDP) is used to represent the triaxial behaviour of concrete. The CDP is an isotropic scalar damage model that uses a potential yield surface in the effective stress space ($\bar{\sigma}$) derived from a combined Drucker–Prager and Rankine representation (Equation 1). The plastic volume expansion is not proportional to the increase in stresses (i.e. non-associative flow rule (Equation 2)). The plastic yield surface is dependent on several parameters, such as dilation angle of the material ϕ, eccentricity of the plastic surface ϵ, material strengths and effective stresses (Equation 3). The constitutive model requires a set of material functions: uniaxial stress–strain relationships and related scalar damage ratios (Equation 4 where i represents compression or tension). A simple bi-linear elasto-plastic relationship for steel is used.

1. $$G = [(\in f_{ct} \tan\phi)^2 + \bar{q}^2]^{1/2} - \bar{p}\tan\phi$$

2. $$\tilde{\varepsilon}_c^{pl} = \lambda \frac{\partial G(\bar{\sigma})}{\partial \bar{\sigma}}$$

3. $$\bar{\sigma}_i = \frac{\sigma_i}{1 - d_i}$$

4. $$\sigma_i = (1 - d_i) E_c (\varepsilon_i - \tilde{\varepsilon}_i^{pl})$$

Validation model

In order to set the material parameters, the numerical model was validated for specimen DB5 tested previously by the authors (Bompa and Oneț, 2011). The flat slab depicted in Figure 5 measured 1·5 m by 1·5 m, was 170 mm thick and had no shear reinforcement. The connection comprised a stub column of 300 mm by 300 mm cross-section and 600 mm height. The specimen was tested upside down with load introduction directly to the column through a 3D pinned joint. The top and bottom reinforcement consisted of 10 mm ribbed bars with a yield strength of 583 MPa. The mean concrete compressive cube strength determined by means of material tests was $f_{c,cube} = 43{\cdot}9$ MPa. The cylinder compressive (35·1 MPa) strength was computed by accounting a correspondence factor between cylinder and cube strength of 0·8 and the concrete elastic modulus was computed according to Model Code 2010 (MC2010) provisions (fib, 2012). The tensile strength determined by means of indirect splitting tests was 2·12 MPa. The clear concrete cover was 15 mm on both top and bottom faces.

Three-dimensional models for RC flat slabs adopt eight-noded brick elements for concrete members and load transfer plates in conjunction with 3D wire elements for the reinforcement. The slab was linearly restrained through reaction plates with the corners free to lift. The moment span on both orthogonal directions was 1450 mm. A mesh sensitivity study indicated a notable influence on the simulated behaviour. Good agreement

Author(s)	No. of specimens	d_{min}–d_{max}: mm	ρ_{min}–ρ_{max}: %	$f_{c,min}$–$f_{c,max}$: MPa	$f_{y,min}$–$f_{y,max}$: MPa	V_{test}/V_{calc}									
						Equation 13		Equation 14		Eurocode 2 (Equation 17a)		ACI 318-14 (Equation 18)		MC2010 (LoA2) ((Equation 19a)	
						Average	CoV	Average	CoV	Average	CoV	Average	CoV	Average	CoV
Al-Yousif and Regan (2003)	2	80	0·9	27·5–29·0	472	1·16	0·06	1·28	0·07	0·91	0·12	1·06	0·12	0·99	0·20
Base (fib, 2001)	20	102–124	1·0–1·9	13·3–39·9	255–432	1·00	0·16	0·99	0·16	1·00	0·15	1·46	0·18	1·06	0·21
Elstner and Hognestad (1956)	14	114–118	1·2–3·0	10·7–39·9	321–409	1·04	0·11	1·03	0·13	1·03	0·09	1·62	0·16	1·16	0·14
EPFL[b]	12	96–456	0·3–1·6	25·7–67·0	480–577	0·96	0·16	0·92	0·16	1·02	0·08	1·18	0·25	1·09	0·10
ETHZ[c]	3	143–294	1·2–1·5	27·1–35·5	515–577	0·95	0·09	0·92	0·11	1·03	0·05	1·47	0·09	1·02	0·22
Bompa and Oneț (2011) and Gosav *et al*. (2013)	4	155–217	0·5–1·4	17·5–35·11	465–583	1·00	0·17	0·94	0·17	1·05	0·14	1·29	0·25	1·02	0·23
Hallgren (1996)	6	194–201	0·6–1·2	81·4–103	596–643	0·93	0·04	0·89	0·06	0·99	0·04	1·11	0·06	0·93	0·06
Hegger *et al*. (2009)	6	395	0·9	21·1–36·4	552	1·12	0·15	0·95	0·15	1·24	0·15	1·54	0·16	1·10	0·17
Inacio *et al*. (2013)	4	102–105	0·9–1·5	35·9–130	493–523	1·04	0·04	1·07	0·04	0·89	0·03	0·99	0·11	0·85	0·05
Kinnunen and Nylander (1960)	10	117–128	0·8–2·1	24·3–31·0	436–461	0·96	0·10	0·95	0·12	1·00	0·09	1·59	0·15	1·01	0·12
Mongi (1990)	16	78	1·5–2·9	21·0–33·4	380–480	1·01	0·14	1·03	0·14	0·99	0·14	1·91	0·17	1·10	0·18
Ladner (1998) and Ladner *et al*. (1977)	7	80–240	1·2–1·8	27·6–36·7	528–550	1·13	0·13	1·11	0·16	1·06	0·14	1·59	0·11	1·09	0·11
Marzouk and Hussein (1991) and Rizk *et al*. (2011)	19	90–313	0·5–2·4	40–80	400–490	1·02	0·12	1·00	0·11	0·99	0·10	1·19	0·26	0·95	0·19
McGill[a]	11	100–300	0·8–1·9	30·1–67·1	434–488	0·99	0·11	1·00	0·13	0·95	0·15	1·19	0·11	0·91	0·10
Moe (1961)	14	114	1·1–2·6	19·5–33·4	328–483	1·14	0·16	1·09	0·17	1·15	0·17	1·91	0·11	1·45	0·19
Oliveira *et al*. (2004)	10	106–109	1·1	54·0–67·0	479	1·07	0·05	1·10	0·07	0·90	0·06	1·04	0·17	0·92	0·13
Ramadane (1996)	11	98–102	0·6–1·3	26·5–97·2	550–650	1·01	0·13	0·99	0·13	1·05	0·10	1·66	0·10	1·16	0·11
Regan (1986)	11	64–200	0·8–1·2	21·6–35·7	480–530	1·02	0·07	1·05	0·10	0·97	0·05	1·27	0·09	1·23	0·19
Tomaszewicz (1993)	13	88–275	1·5–2·6	64·1–118	500	1·02	0·07	0·92	0·07	1·05	0·08	1·47	0·08	1·10	0·10
Urban *et al*. (2013)	3	218–318	0·4	32·5	544–580	1·17	0·09	1·10	0·06	1·61	0·10	1·83	0·11	1·61	0·13
Various[d]	13	100–260	0·6–2·2	21·9–56·1	420–481	0·92	0·09	0·91	0·10	0·98	0·11	1·22	0·29	0·94	0·22
	209					1·02	0·13	1·00	0·14	1·02	0·15	1·44	0·25	1·08	0·21

[a]Ghannoum (1998), McHarg (1997) and Kevin (2000)
[b]Guandalini *et al*. (2009), Guidotti (2010), Krueger (1999) and Sagaseta *et al*. (2011)
[c]Heinzmann (2012) and Pralong (1982)
[d]Beutel (2002), Birkle and Digler (2008), Broms (1990), Caldentey *et al*. (2013), Moreno and Sarment (2013), Schaefers (1984), Swamy and Ali (1982) and Wörle (2014)
CoV: coefficient of variance

Table 1. Database of punching shear tests

between the test and numerical results regarding both stiffness and stress values was found for a mesh size of ≈19 mm, resulting in nine layers of mesh for the slab thickness. The arc length method was used as the integration procedure. In the case of cohesive-brittle materials such as concrete, the internal friction angle β and dilation angle ϕ play a notable role in obtaining a reliable numerical response. A commonly agreed range of values for ϕ is 20–40°. It was observed that the best response was received for a dilation angle of 40°. The other constitutive parameters were also varied, resulting in shape of the deviatoric plane $K_c = 2/3$ and eccentricity of the plastic surface $\epsilon = 0{\cdot}1$.

Figure 5(a) plots the numerical response against the response recorded in the test. The ultimate strength in the numerical simulation was reached due to a localised crushing failure in the stress field formed in the slab near the column region (Figure 5(d)). The first yield of the flexural reinforcement was recorded at 440 kN, which was similar to the value obtained by means of analytical modelling (Muttoni, 2008). The tension damage map shows a flexural-controlled behaviour at early loading stages with the concentration of damage following typical yield line patterns. At failure, the internal damage pattern is represented by a conical shape (Figure 5(c)), resembling the test recorded crack pattern at the top face of the slab (Figure 5(b)).

Parametric investigation

In order to assess the elastic stress fields that develop within interior slab to column connections, a series of eight flat-slab

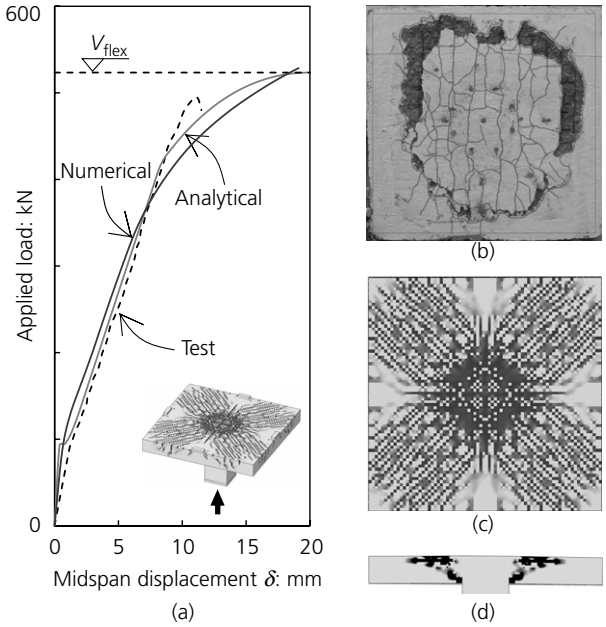

Figure 5. (a) Numerical calibration of test specimen DB5; load–displacement response. (b) Crack pattern on top face of specimen. (c) Tension damage in numerical model. (d) Compression damage in slab section

column connections was examined by varying the slab thickness. The average effective depth of 209 specimens from the literature (Table 1) is 146 mm. Specimen DB5 was used as a reference to validate the numerical model since its effective depth ($d_{DB5} = 145$ mm) was nearly identical to the average value in the database. In the parametric study, the reinforcement ratio, steel yield strength and concrete strength were maintained constant, whereas the thickness was varied (Figure 6). The moment span was maintained constant for all models. Figure 6(b) show the relationship between the studied parameters against the ultimate strength resulting from the Ottosen yield criterion over the numerical response (Ottosen, 1980). The thickness variation from 150 mm to 500 mm showed a proportional increase regarding the inclination of compression stress field (Figure 6(a)) and a decrease in the normalised strength with the increase of slenderness (Figure 6(b)). Due to limited thickness, in thin slabs, the inclination of the compression field is 31°, whereas for thicker slabs it tends to follow a 45° path. For thick slabs, there is less geometrical constraint in the development of the compression stress field. Therefore it is natural to have steeper inclinations.

Ultimate punching shear strength

A novel method to assess the punching shear strength of flat slabs at the connection to interior columns is proposed here. The method was developed from the assumptions that the shear is carried by a 3D strut formed around the column and the concrete characteristic shear transfer actions. The key parameter that controls the punching shear strength is the inclination of the punching shear crack, which increases linearly with the reinforcement ratio and effective depth. The location of the critical section varies with slab geometry and material characteristics. The method disregards the beneficial effect of compressive membrane action and hence it offers a safe estimate. The inclination of the punching shear crack is governed by the stress distribution in the connection region. The punching shear strength, evaluated at the conical failure surface, is governed by the amount of shear carried through the cracked interface. The crack inclination angle and the amount of shear carried through the failure surface are dependent on the geometry of the member (depth, slenderness, column dimension to slab thickness) and the characteristics of the structural key parameters (material strengths, aggregate distribution and dimension, reinforcement layout etc.).

The transfer of residual stresses through the fracture process zone is not accounted for. The method proposed here was validated with a series of isolated specimens tested in various support and load conditions and is limited to interior connections without shear reinforcement.

Considering a variable inclination of the punching shear crack, the proposed method offers better control compared with existing design guidelines since it accounts for a higher variety of

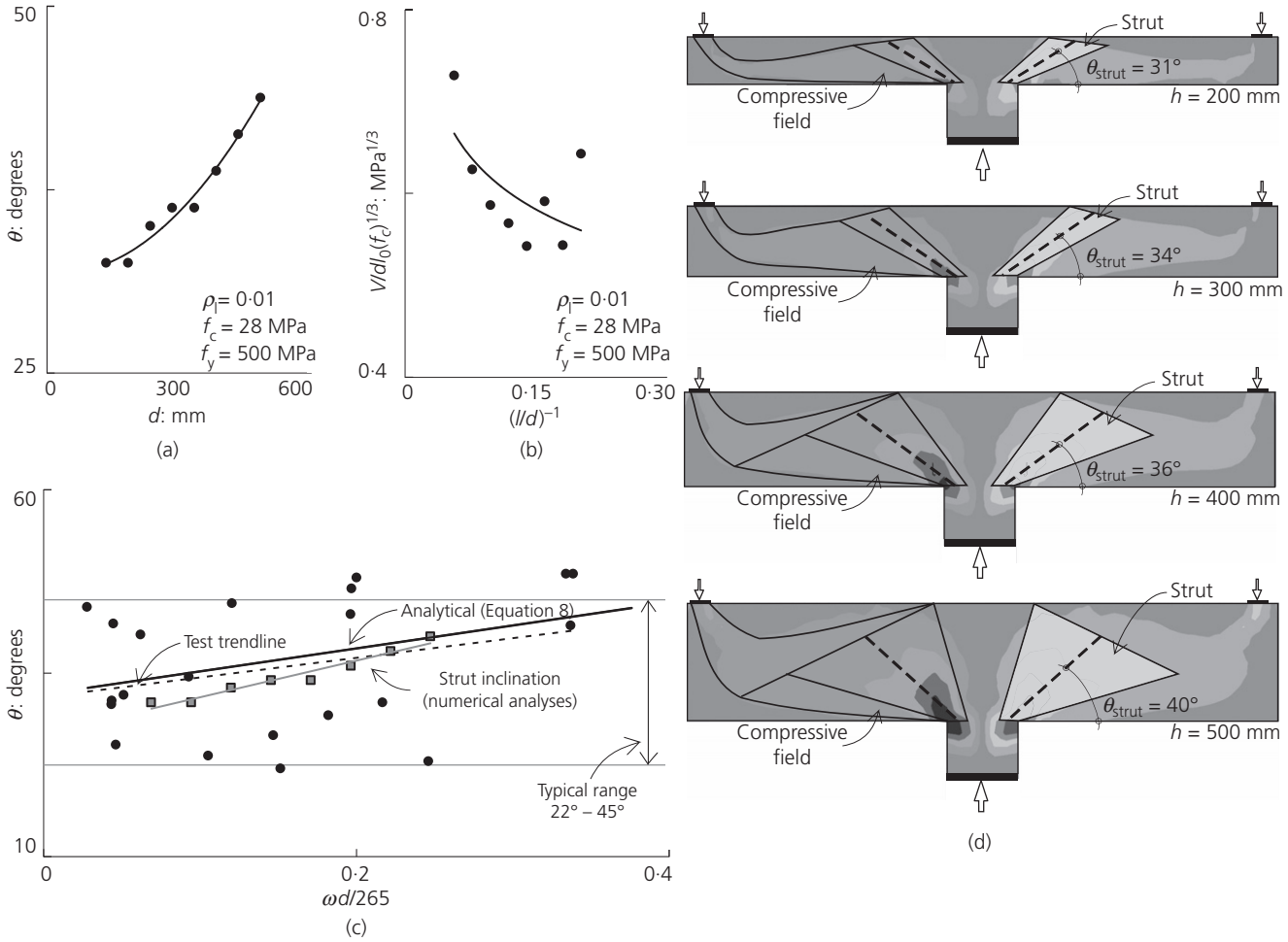

Figure 6. (a) Relationship between strut inclination and effective depth of the slab. (b) Normalised punching shear strength related to slab slenderness. (c) Relationship between crack inclination (reported in tests), strut inclination (by means of numerical analyses) and analytical prediction (Equation 8). (d) Finite-element analysis plots and assumptions for strut inclination in relation to slab thickness.

structural parameters. The method is applicable to the assessment of the punching shear strength of flat slabs connected to interior columns with circular or rectangular cross-sections without shear reinforcement. The method proposed was validated with 209 tests on isolated specimens reported in the literature (suspended slabs and footings) (Al-Yousif and Regan, 2003; Bazant and Cao, 1987; Bernaert and Puech, 1966; Beutel, 2002; Birkle and Digler, 2008; Bompa and Oneț, 2011; Broms, 1990; Caldentey *et al.*, 2013; Elstner and Hognestad, 1956; Ghannoum, 1998; Guandalini *et al.*, 2009; Gosav *et al.*, 2013; Guidotti, 2010; Hallgren, 1996; Hegger *et al.*, 2009; Heinzmann *et al.*, 2012; Inacio *et al.*, 2013; Kevin, 2000; Kinnunen and Nylander, 1960; Krueger, 1999; Ladner, 1998; Ladner *et al.*, 1977; Marzouk and Hussein, 1991; McHarg, 1997; Menetrey, 2002; Moe, 1961; Mongi, 1990; Moreno, 2013; Muttoni, 2008; Muttoni and Fernandez Ruiz, 2012; Oliveira *et al.*, 2004; Pralong, 1982; Ramadane, 1996; Regan, 1986; Rizk *et al.*, 2011; Sagaseta *et al.*, 2011; Schaefers, 1984; Swamy and Ali, 1982; Tomaszewicz, 1993; Urban *et al.*, 2013; Wörle, 2014). The condensed results can be found in Table 1 and the extended data for calculation in the Appendix.

Prediction method

A prediction method was developed based on previous findings by means of numerical analyses, analytical investigations on the existing test database (Table 1) and test observations carried out by the authors (Bompa and Oneț, 2011; Gosav *et al.*, 2013). The method has, as its basis, the concept of variable inclination of the unique punching shear crack (Figure 7(a)). Considering that the angle of the crack is defined by the line that connects the root of the column to the intersection of the crack with the flexural reinforcement, the reported angles as a result of saw cuts through the slab on 21 tests vary from 20° to 49° (Beutel, 2002; Guandalini *et al.*, 2009; Hallgren, 1996; Hegger *et al.*, 2009; Heinzmann *et al.*, 2012; Ladner, 1998; Pralong, 1982) (e.g. Figure 3(b)). In agreement

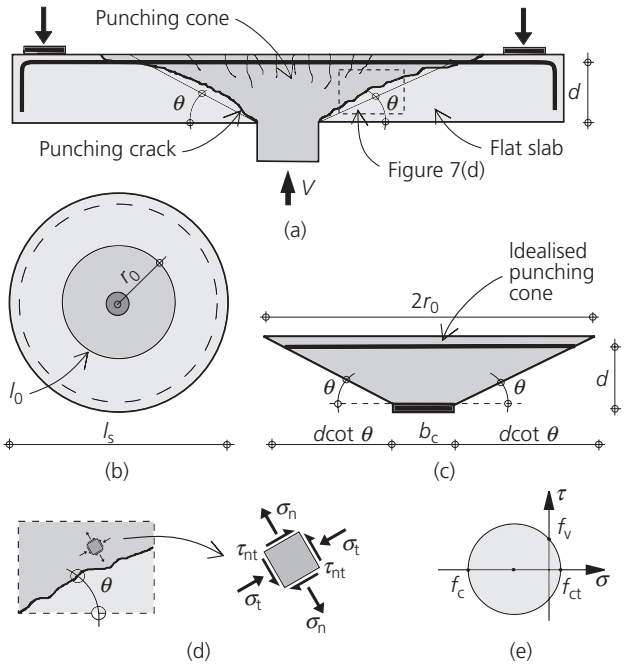

Figure 7. (a) Typical punching shear failure for flat slabs near column region. (b) In-plane dimensions of slab. (c) Dimensions of the punching cone. (d) State of stresses above the punching shear crack. (e) Mohr circle for concrete strengths

with the results in Figures 6(c) and 6(d), a correlation between the inclination of the compression stress field (numerical) and average crack inclination reported from tests was found (Equation 5). The predicted crack angle depends on the reinforcement ratio ρ, the effective depth d and the material strength ratio f_y/f_c. The influence of slab thickness on crack inclination angle was calibrated against the average effective depth of the slabs with available reported saw cuts (i.e. $d_{avg} = 265$ mm).

5a. $$\tan\theta = 0.6 + \omega\left(\frac{d}{265}\right)^{1/2}$$

5b. $$\omega = \rho f_y / f_c$$

The punching shear crack formed at the centreline of the compression field, connecting the root of the column to the tension face of the slab, produces a conical body that dislocates from the slab (Figures 7(a) and 7(c)). The resulting punching cone is defined geometrically by the column dimension b_c, bending effective depth d and inclination angle of the crack θ. Assuming that the frustum of the cone has a circular shape at both lower and upper bases, the perimeter of the punching shear crack at the centroid of the flexural reinforcement is given by l_0 (Equation 6). In the case of rectangular columns, its dimension can be estimated by considering a circular column with the same area ($b_c = 2b_{c,r}/\pi^{1/2}$). For rectangular columns with a column dimension ratio different from one, the column dimension can be regarded as the square root of the product of the two dimensions $b_{c,r} = (b_{c,1} \times b_{c,2})^{1/2}$. The root of the column and the circular line at the top face of the slab represents the boundary between two rigid bodies that separate at failure (i.e. punching cone and slab). The area of the failure surface is the slant of the frustum of the cone (Equation 7).

6. $$l_0 = \pi(b_c + 2d\cot\theta)$$

7. $$A_{pc} = \pi d(b_c + d\cot\theta)/\sin\theta$$

Significant shear is transferred from the slab to the column through the inclined compression stress field (Figure 2(c)). Accounting for the state of stress in Figure 7(d), the increase in strut stresses results in tension in the normal direction (σ_n). Considering that concrete is a Coulomb material, the typical failure modes are sliding and separation (Nielsen, 1999). Prior to separation of the two bodies, concrete can withstand a stress equal to the tensile strength in the normal direction to the crack ($\sigma_n = f_{ct}$). The shear strength f_v in the region can be predicted using the Mohr–Coulomb criterion (Figure 7(e), Equation 10)). However, the assumptions are valid for plain concrete. In the case of RC, the typical behaviour is disturbed. The influence is accounted for by considering the cube root of f_v. In conjunction with the slenderness of the punching cone λ (Equation 9), the contribution of the interlocking aggregates and the transfer through the compressive zone are estimated by Equation 8.

Equation 11 is an application of the findings reported by Ince *et al.* (2007) regarding the shear response of the embedded dowels in concrete, which relates the strength of the dowel to the reinforcement ratio ρ, its yield strength $f_{y,}$, concrete strength f_c and aggregate size d_g (size effect). In this paper, the size effect is accounted for by the factor ξ (Equation 16), which is dependent on the effective depth and the fractal parameter of the concrete (characteristic length l_{ch}). Equation 11 is modified from the original form by disregarding the size effect and integrating the influence of dowel bending over the critical section ($l_0 d$). By using the reinforcement ratio and a fraction of the yield strength of the flexural reinforcement, in its general form Equation 11 takes into account the influence of flexural strength on the punching shear strength.

The punching shear strength of a slab at interior columns is given by Equation 13. A condensed form of the proposed method is also available. Considering that the relationship between the cube root of the shear strength and the cube root of the concrete strength is given by the equality in Equation 12 and the ratio $A_{pc}/l_0 = 1{\cdot}25d$ (on average, considering the

available database) Equation 13 can be condensed into Equation 14.

$$V_1 = \lambda A_{pc}(f_v)^{1/3} \quad (8)$$

$$\lambda = d/(b_c + 2d\cot\theta) \quad (9)$$

$$f_v = (f_c f_{ct})^{1/2} \quad (10)$$

$$V_2 = \rho_l(f_y)^{1/3}(f_c)^{1/3} l_0 d \quad (11)$$

$$(f_v)^{1/3} \cong \frac{2}{3}(f_c)^{1/3} \quad (12)$$

$$V_R = (V_1 + V_2)\xi \quad (13)$$

$$V_R = 2\pi d(f_c)^{1/3}[0.4d + \rho_l(f_y)^{1/3} r_0]\xi \quad (14)$$

$$r_0 = d\cot\theta + b_c/2 \quad (15)$$

$$\xi = 0.75 + (d/l_{ch})^{-0.2} \quad (16)$$

Validation of the method

Figures 8(a) and 8(b) respectively show the predictions of Equations 13 and 14 considering the data listed Table 1. The ratio of reported strength to predicted strength (V_{test}/V_{calc}) is plotted against the ratio of the reported strength and the specimen's flexural strength (V_{test}/V_{flex}). The database consists of 209 tests presenting a wide range of mechanical and geometrical parameters (55 slabs with circular columns and 154 slabs with rectangular columns of which 141 were square). The test specimens had various structural parameters. The flexural reinforcement ratio (ρ) varied between 0·33% and 3·00%. The compressive concrete strength, obtained on cylinder specimens, was 10·7–130·1 MPa, whereas the yield strength of bending reinforcement varied from 255 MPa to 720 MPa. The in-plane dimensions varied from 0·73 m to 6·0 m and the slab thickness varied from 80 mm to 500 mm. The average effective depth (d_{avg}) of all the specimens in the database was 146 mm and the average reinforcement ratio was 1·30%. The centralised values are listed in Table 1 and the complete database is given in the Appendix.

Comparison with codified approaches

The codified rules propose different relationships to assess the punching shear strength. The calculations are made considering a critical section that lies at a certain distance from the face of the column. The European design code Eurocode 2 (CEN, 2004) uses a critical perimeter at $2d$ (Equation 17a) whereas the American design code ACI 318-14 (ACI, 2014) (Equation 18) and MC2010 (fib, 2012) (Equation 19a) define the critical section at $d/2$. In all the above methods, the punching shear strength is a function of the concrete strength f_c, effective depth d and the critical perimeter b_0. Eurocode 2 and MC2010 account for the influence of the flexural capacity and size effect on the punching shear strength (Equations 17b and 19b). MC2010 considers that the governing parameter in assessing the punching strength is the rotation of the slab ψ (Equation 19c).

$$V_{R,EC2} = 0.18\xi(100\rho_l f_c)^{1/3} b_0 d \quad (17a)$$

$$\xi = 1 + (200/d)^{1/2} \quad (17b)$$

$$V_{R,ACI} = 0.33 b_0 d (f_c)^{1/2} \quad (18)$$

$$V_{R,MC2010} = k_\psi (f_c)^{1/2} b_0 d \quad (19a)$$

$$k_\psi = 1/(1.5 + 0.6\psi d k_{dg}) \quad (19b)$$

$$\psi = 1.5\frac{r_{s,i} f_{yd}}{d\ E_s}\left(\frac{m_{sd,i}}{m_{rd,i}}\right)^{3/2} \quad (19c)$$

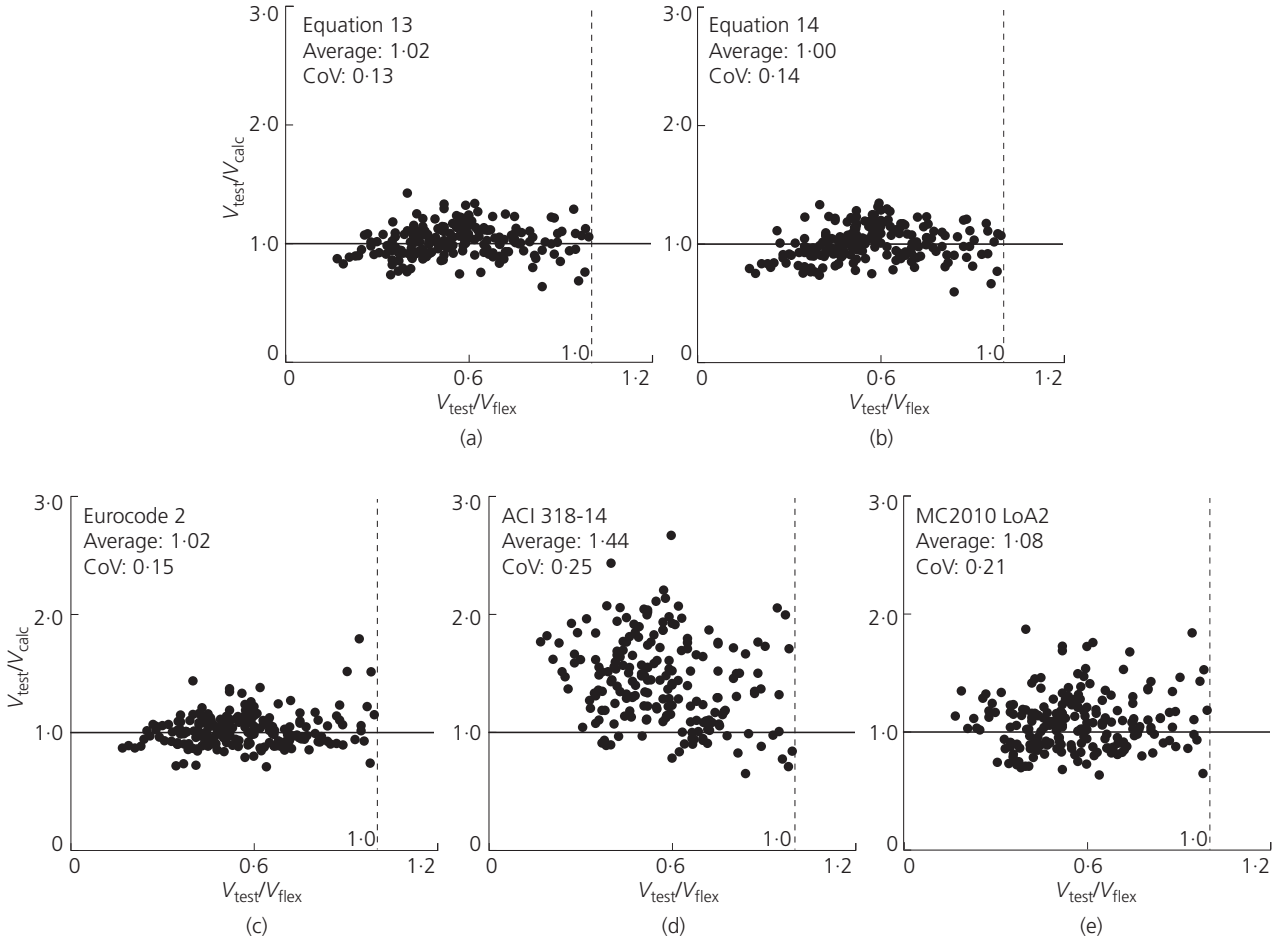

Figure 8. Prediction of ultimate punching shear strength according to: (a) the proposed method (Equation 13); (b) the proposed method (Equation 14); (c) Eurocode 2; (d) ACI 318-14; (e) MC2010 (LoA2)

In these equations, k_{dg} is a factor that is dependent on the maximum aggregate dimension ($k_{dg} = 32/(16 + d_g)$), r_s is the distance between zero moment and load application point, d is the effective depth, f_{yd} is the design yield strength of bending reinforcement, E_s is the modulus of elasticity for rebars, m_{sd} is the average bending moment acting in the support strip and m_{rd} is the flexural strength per unit length in the support strip.

The results in Table 1 show the punching shear strength predictions V_{calc} of the codified approaches and the proposed method in relation to the reported strength V_{test} on a database of 209 isolated interior flat-slab column connections. The specimens are grouped on the basis of the author or research group that carried out the investigation. The table plots the number of specimens per author/group, the minimum and maximum values of effective depth d, flexural reinforcement ratio ρ, concrete compressive strength f_c, steel yield strength f_y and the statistical parameters (average and coefficient of variance (CoV)) for the reported to predicted ultimate punching shear strengths V_{test}/V_{calc}. The case when the reported strength is smaller than the predicted strength is represented by a V_{test}/V_{calc} value less than 1·00. The statistical parameters are plotted for each group of specimens. All the reported data, including the ultimate strength V_{test}, structural parameters of each specimen and statistical parameters as result of computed predictions, are given in the Appendix.

The proposed method (Equation 13) shows an average V_{test}/V_{calc} of 1·02 and a CoV of 0·13 (Figure 8(a)), while the condensed form (Equation 14) shows a V_{test}/V_{calc} ratio of 1·00 and a slightly higher CoV of 0·14 (Figure 8(b)). In both cases, the prediction offered by the proposed method offer good predictions of the ultimate punching shear strength. Figure 8 also shows a comparison between

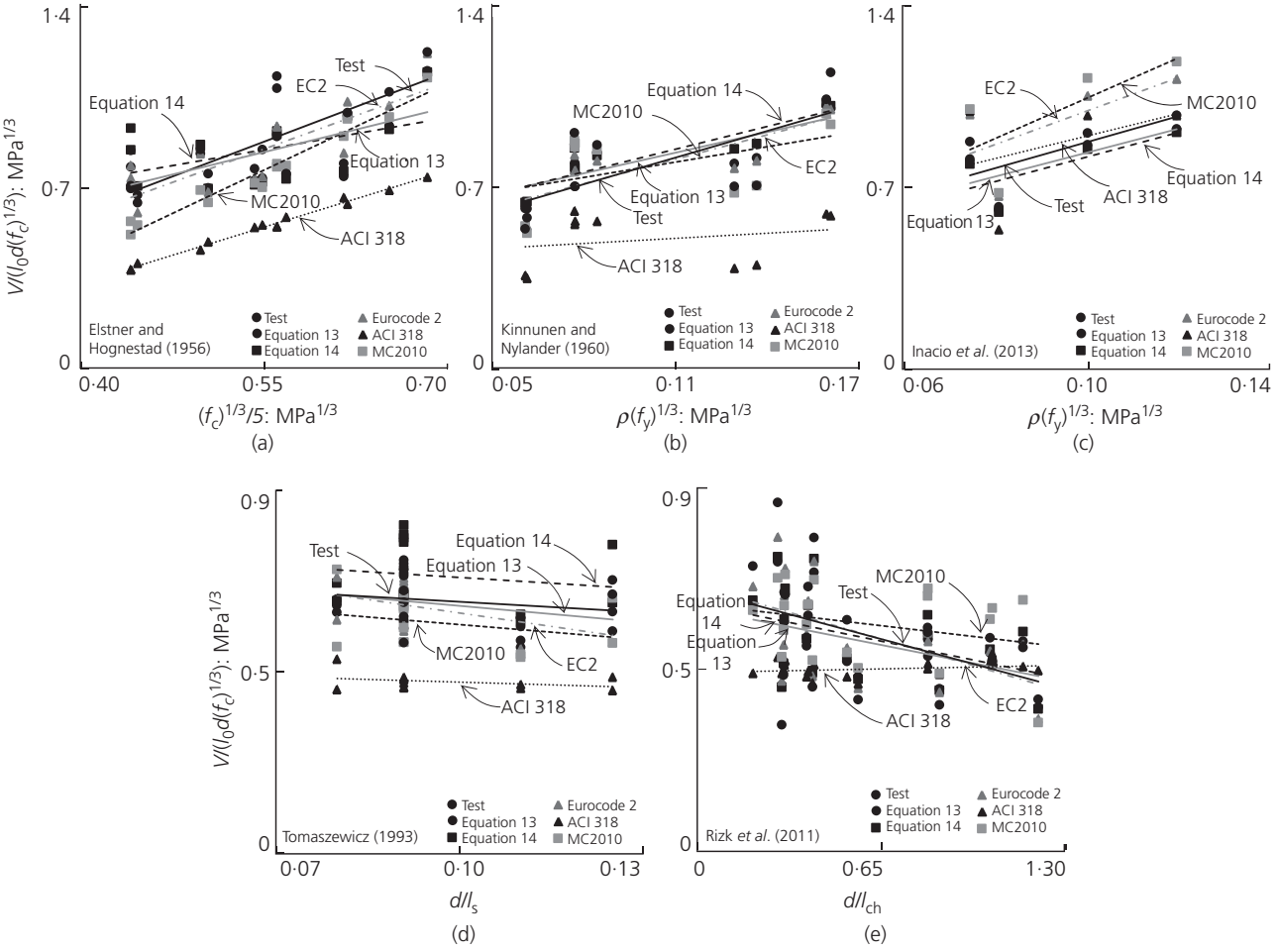

Figure 9. Predictions and trend curves for a series of selected tests according to the proposed model and current design procedures: (a) concrete strength; (b) reinforcement ratio for normal-strength concrete; (c) reinforcement ratio for high-strength concrete; (d) slenderness of the slab; (e) size effect (concrete fractal parameter)

the condensed form (Equation 14) and current design codes (Eurocode 2 (Equation 17a), ACI 318-14 (Equation 18) and MC2010 level II of approximation (LoA2) (Equation 19a). The proposed Equation 14 shows notable outcomes regarding the statistical parameters (average and CoV). Eurocode 2 (CEN, 2004) shows a similar CoV (0·15) and average (1·02) with a slight tendency to overestimate the ultimate strength for low reinforcement ratios (i.e. large V_{test}/V_{flex}). ACI 318-14 (ACI, 2014) offers conservative predictions (CoV of 0·25 and average of 1·44). The scatter points tend to reproduce the decreasing trend of the computed values, leading to higher predicted values than those reported in tests. For a similar level of refinement, MC2010 (LoA2) offers slightly more conservative results compared with the proposed method. However, a higher degree of refinement is available in MC2010 and hence better statistical parameters may be obtained (Muttoni and Fernandez Ruiz, 2012).

Parametric comparisons

This section compares the proposed method and the existing guidelines with regard to a series of key structural parameters. Figure 9(a) presents the capability of the proposed method to follow the contribution of concrete to the punching shear strength. Elstner and Hognestad (1956) carried out a series of tests on rectangular slabs in which the varying parameter was concrete strength. The figure shows that the proposed method follows the relationship between concrete strength and normalised strength in a satisfactory way.

Figures 9(b) and 9(c) plot the relationship between the flexural characteristics of the slab and the ultimate strength (in normalised values) of normal-strength concrete (Kinnunen and Nylander, 1960) and high-strength concrete (Inacio *et al*., 2013). Variation of the reinforcement ratio from low to high (0·54% to 2·10% and 0·94% to 1·49% respectively) reveals excellent agreement between the predicted and reported

strengths for both extreme cases of concrete strength (≈29·3 MPa and ≈129 MPa respectively). The other design methods show a similar response, but ACI 318-14 shows a contrasting trend. The influence of the reinforcement ratio and steel yield strength is estimated by a nearly constant line due to the fact that formulation of the code rules of ACI 318-14 does not include flexural characteristics of the slab.

The influence of the slenderness of the slab is best captured by Equation 13 (Figure 9(d)), which closely predicts the ultimate punching strength from the tests reported by Tomaszewicz (1993). The size effect is emphasised by means of the fractal parameter of concrete (l_{ch}) and effective depth (d) from tests carried out by Marzouk and Hussein (1991) and Rizk *et al*., (2011) (Figure 9(e)). Although all the results show a similar trend of the normalised strength in relation to d/l_{ch}, the actual behaviour is better anticipated by the proposed method (Equations 13 and 14) and Eurocode 2 for small fractal values (l_{ch}).

Concluding remarks

A method is proposed to evaluate the punching shear strength of RC flat slabs without shear reinforcement at the connection to interior columns. The method is based on the assumption that punching shear strength is controlled by the inclination of a unique punching shear crack that produces a conical failure surface. The inclination angle is variable and therefore the location of the critical section is not predefined. The method was verified on a database of 209 tests on isolated specimens reported in literature. It shows notable agreement with the test results regarding both the influence of key structural parameters and statistical parameters compared with codified provisions (average and CoV). The method offers safe estimates since the beneficial effect of compressive membrane action is disregarded. Taking account of information obtained in tests (Bompa and Oneț, 2011; Gosav *et al*., 2013) and the findings from the numerical and analytical investigations, the conclusions can be summarised as follows.

- According to the proposed method, punching shear failure is described by the development of a unique punching shear crack with variable inclination, producing a conical failure surface. The parameters that control crack inclination are the flexural reinforcement ratio, slab thickness and concrete and reinforcement steel strengths. The inclination of the crack determines the amount of shear carried by specific concrete shear transfer actions.
- Considering experimental observations and reported cross-sectional crack patterns, the cracks tend to form at flatter angles for low reinforcement ratios and at steeper ones for high reinforcement ratios.
- The numerical investigations show that an increase in slab thickness produces a proportional increase in the angle of the compression stress field and consequently in the inclination of the punching shear crack.
- Based on the reported results in the test database, the structural parameters that control the behaviour of flat slabs at ultimate state are flexural characteristics (proportional increase of punching strength for an increase in reinforcement ratio), slenderness of the slab (increase in strength with decrease in slenderness) and concrete strength (decreasing normalised punching shear strength with increasing concrete strength for low and moderate reinforcement ratios).
- The punching shear strength of flat slabs without shear reinforcement at the connection to interior columns is calculated as a function of the crack inclination (θ), effective depth (d), concrete strength (f_c), reinforcement ratio and strength (ρ and f_y) and column dimension (b_c). The method accounts for the characteristic concrete size effect by considering the ratio of effective depth d to fractal parameter l_{ch}.
- Accounting for a variable inclination of the crack, the proposed method offers good predictions of the ultimate punching shear strength for extreme geometrical and material configurations such as low reinforcement ratios and high-strength concretes. The results, based on a series of 209 tests, show an average of 1·00 and CoV of 0·14 for the condensed form of the method (Equation 14) and an average of 1·02 and a CoV of 0·13 for the extended form (Equation 13).
- The European provision Eurocode 2 (CEN, 2004) shows a similar CoV and a slight tendency to overestimate the ultimate strength for low reinforcement ratios (i.e. large values of V_{test}/V_{flex}). The American design guideline ACI 318-14 (ACI, 2014) offers conservative predictions (CoV of 0·25 and average of 1·44). The scatter points tend to reproduce the decreasing trend of the computed values, leading to higher predicted values than those reported in tests. For a similar level of refinement, Model Code 2010 (LoA2) (fib, 2012) offers slightly more conservative results than the proposed method (average of 1·08 and CoV of 0·21).

Acknowledgements

The financial support of ESF through the EU-funded project Prodoc at Technical University of Cluj-Napoca, Romania is gratefully acknowledged by the authors (where the early stage of the work was carried out). Additionally, the first author would like to thank to Professor A. R. Marí Bernat and Professor J. M. Bairan García from Universitat Politècnica de Catalunya for their valuable comments and suggestions regarding the work carried out and reported in this paper during the research mobility stage spent at their department.

Appendix

							$V_{R,calc}/V_{u,test}$				
Specimen	d: mm	ρ	f_c: MPa	d_g: mm	f_y: MPa	$V_{u,test}$: kN	Equation 13	Equation 14	Eurocode 2	ACI 318-14	MC2010 (LoA2)
Hallgren (1996)											
HSC0	200	0·008	89·2	18	643	965	0·87	0·80	0·98	1·10	0·91
HSC1	200	0·008	86·7	18	627	1021	1·00	0·97	1·05	1·18	1·02
HSC2	194	0·008	81·4	18	620	889	0·93	0·89	0·97	1·10	0·91
HSC4	200	0·012	87·0	18	596	1041	0·92	0·87	0·93	1·20	0·86
HSC6	201	0·006	103	18	633	960	0·95	0·92	1·01	1·00	0·98
N/HSC8	198	0·008	90·2	18	631	944	0·93	0·90	0·97	1·08	0·88
Tomaszewicz (1993)											
ND65-1-1	275	0·015	64·1	16	500	2050	1·09	0·96	1·15	1·48	1·15
ND65-2-1	200	0·017	70·0	16	500	1200	1·05	0·94	1·09	1·55	1·23
ND95-1-1	275	0·015	83·5	16	500	2250	1·11	0·99	1·15	1·43	1·19
ND95-1-3	275	0·025	89·7	16	500	2400	0·95	0·84	1·01	1·47	1·01
ND95-2-1	200	0·017	88·0	16	500	1100	0·91	0·82	0·92	1·27	0·93
ND95-2-1D	200	0·017	86·5	16	500	1300	1·08	0·96	1·10	1·51	1·19
ND95-2-3	200	0·026	89·3	16	500	1450	1·01	0·91	1·05	1·66	1·18
ND95-2-3D	200	0·026	80·1	16	500	1250	0·90	0·80	0·94	1·51	1·03
ND95-2-3D+	200	0·026	97·8	16	500	1450	0·98	0·88	1·02	1·59	1·12
ND95-3-1	88	0·018	84·9	16	500	330	1·02	1·00	0·91	1·30	0·89
ND115-1-1	275	0·015	112	16	500	2450	1·10	0·98	1·14	1·34	1·16
ND115-2-1	200	0·017	119	16	500	1400	1·05	0·94	1·06	1·39	1·12
ND115-2-3	200	0·026	108	16	500	1550	1·01	0·91	1·06	1·62	1·16
Marzouk and Hussein (1991) and Rizk *et al*. (2011)											
I.NS1	95	0·0147	42·0	20	490	320	1·15	1·14	1·08	1·61	1·18
I.HS1	95	0·0049	67·0	20	490	178	0·76	0·77	0·74	0·71	0·65
I.HS2	95	0·0084	70·0	20	490	249	0·94	0·94	0·85	0·97	0·80
I.HS7	95	0·0193	74·0	20	490	356	1·00	0·98	0·91	1·35	0·93
I.HS3	95	0·0147	69·0	20	490	356	1·13	1·12	1·01	1·39	1·06
I.HS4	90	0·0237	66·0	20	490	418	1·21	1·19	1·11	1·80	1·28
II.HS5	125	0·0064	68·0	20	490	365	0·94	0·91	0·94	0·98	0·86
II.HS7	120	0·0094	74·0	20	490	489	1·22	1·20	1·14	1·33	1·16
II.HS8	120	0·0111	69·0	20	490	436	1·04	1·01	0·98	1·23	0·94
II.HS9	120	0·0161	74·0	20	490	543	1·12	1·08	1·06	1·48	1·07
II.HS10	120	0·0233	80·0	20	490	645	1·12	1·07	1·08	1·69	1·16
NS2	218	0·0073	40·0	19	400	882	0·87	0·88	0·93	0·90	0·83
HS2	218	0·0073	64·7	19	400	1023	0·90	0·91	0·92	0·82	0·82
HS3	263	0·0144	65·4	19	400	2090	1·01	1·02	0·97	0·96	0·78
NS3	313	0·0157	40·0	19	400	2234	0·92	0·90	0·93	1·04	0·74
HSS1	268	0·0050	76·0	19	460	1722	1·06	1·07	1·15	0·84	1·18
HSS3	263	0·0142	65·0	19	460	2090	1·08	1·06	1·07	1·13	0·92
NSS1	313	0·0158	40·0	19	460	2234	0·98	0·93	1·00	1·20	0·86
JSS4	313	0·0158	60·0	19	460	2513	0·97	0·93	0·98	1·10	0·81
Regan (1986)											
I/1	77	0·0120	25·4	10	500	194	1·07	1·11	0·97	1·37	1·28
I/2	77	0·0120	23·1	10	500	176	0·99	1·02	0·91	1·30	1·16
I/3	77	0·0092	27·1	10	500	194	1·14	1·21	1·04	1·32	1·46
I/4	77	0·0092	31·9	10	500	194	1·10	1·17	0·98	1·22	1·33
I/5	79	0·0075	27·8	10	480	165	0·97	1·04	0·91	1·08	1·17
I/6	79	0·0075	21·6	10	480	165	1·02	1·09	0·99	1·22	1·35
I/7	79	0·0080	30·0	10	480	186	1·07	1·14	0·98	1·17	1·68

Table A1. (continued on next page)

Specimen	d: mm	ρ	f_c: MPa	d_g: mm	f_y: MPa	$V_{u,test}$: kN	$V_{R,calc}/V_{u,test}$				
							Equation 13	Equation 14	Eurocode 2	ACI 318-14	MC2010 (LoA2)
II/1	200	0·0100	34·4	20	530	825	0·94	0·90	1·00	1·18	0·86
II/2	128	0·0100	32·9	20	485	390	1·02	0·98	1·04	1·40	1·09
II/3	128	0·0100	33·9	10	485	365	0·95	0·92	0·97	1·29	0·89
II/6	64	0·0100	35·7	5	480	105	0·96	0·95	0·89	1·44	1·27
Moe (1961)											
S1-60	114	0·0110	22·1	38	399	389	1·34	1·29	1·38	2·07	1·76
S2-60	114	0·0150	21·0	38	399	356	1·15	1·09	1·16	1·94	1·41
S3-60	114	0·0200	21·5	38	399	364	1·08	1·01	1·07	1·96	1·33
S4-60	114	0·0260	22·6	38	399	334	0·89	0·83	0·88	1·76	1·11
S1-70	114	0·0110	23·3	38	483	393	1·33	1·28	1·37	2·03	1·73
S3-70	114	0·0200	24·1	38	483	378	1·08	1·01	1·07	1·92	1·32
S4-70	114	0·0260	33·4	38	483	374	0·88	0·83	0·87	1·62	1·03
S4-70A	114	0·0260	19·5	38	483	312	0·87	0·79	0·87	1·77	1·13
S5-60	114	0·0110	21·1	38	399	343	1·19	1·15	1·24	1·87	1·49
S5-70	114	0·0110	21·9	38	483	378	1·29	1·23	1·34	2·02	1·69
R1	114	0·0140	25·3	10	328	312	0·98	0·95	0·98	1·55	1·23
R2	114	0·0140	26·2	10	328	394	1·23	1·20	1·22	1·92	1·72
H1	114	0·0110	24·8	38	328	372	1·25	1·22	1·27	1·87	1·53
M1A	114	0·0150	19·8	38	481	433	1·42	1·33	1·44	2·43	1·87
Kinnunen and Nylander (1960)											
IA15a-5	117	0·0080	27·6	32	441	255	0·87	0·84	0·96	1·50	0·98
IA15a-6	118	0·0080	25·4	32	454	275	0·94	0·90	1·05	1·66	1·11
IA15c-11	121	0·0180	31·0	32	436	334	0·87	0·81	0·88	1·76	1·00
IA15c-12	122	0·0170	28·4	32	439	332	0·89	0·83	0·91	1·81	1·04
IA30a-24	128	0·0100	25·6	32	456	430	1·05	1·07	1·10	1·50	1·03
IA30a-25	124	0·0110	24·3	32	451	408	1·04	1·05	1·08	1·52	1·02
IA30c-30	120	0·0210	29·2	32	436	491	1·02	1·01	1·03	1·74	1·06
IA30c-31	119	0·0210	29·2	32	448	540	1·14	1·13	1·14	1·93	1·21
IA30e-34	120	0·0100	26·5	32	461	332	0·89	0·92	0·92	1·23	0·81
IA30e-35	122	0·0100	24·3	32	459	332	0·89	0·90	0·92	1·26	0·82
Elstner and Hognestad (1956)											
IA-1a	118	0·0115	11·1	25	332	303	0·96	0·91	1·06	1·57	1·16
IA-1b	118	0·0115	19·9	25	332	365	1·06	1·09	1·05	1·41	1·08
IA-1c	118	0·0115	22·9	25	332	356	1·00	1·03	0·98	1·28	0·96
IA-1d	118	0·0115	29·1	25	332	351	0·94	0·97	0·89	1·12	0·83
IA-1e	118	0·0115	16·0	25	332	356	1·08	1·08	1·10	1·54	1·17
IA-2a	114	0·0247	10·7	25	321	334	0·91	0·84	0·96	1·84	1·24
IA-2b	114	0·0247	15·4	25	321	400	1·02	0·98	1·02	1·84	1·23
IA-2c	114	0·0247	29·5	25	321	467	1·01	1·01	0·96	1·55	1·02
IA-7b	114	0·0247	22·0	25	321	512	1·21	1·20	1·16	1·97	1·37
IIA-4	118	0·0115	20·6	25	332	400	1·15	1·17	1·14	1·52	1·21
IIA-5	114	0·0247	22·0	25	321	534	1·25	1·23	1·21	2·06	1·45
VIII B-9	114	0·0200	34·7	25	341	505	1·14	1·16	1·05	1·55	1·10
VIII B-11	114	0·0300	10·7	25	409	329	0·83	0·75	0·89	1·82	1·35
VIII B-14	114	0·0300	39·9	25	325	578	1·06	1·07	1·00	1·65	1·09
Guandalini *et al*. (2009)											
PG-1	210	0·0150	25·7	16	573	1023	1·07	0·97	1·10	1·55	1·21
PG-3	456	0·0033	31·8	16	520	2153	0·63	0·59	0·92	0·65	1·12
PG-6	96	0·0150	27·1	16	526	236	0·98	0·94	0·94	1·58	1·29
PG-7	100	0·0075	33·7	16	550	241	1·01	0·98	1·06	1·37	1·17
PG-10	210	0·0033	29·5	16	577	540	0·68	0·66	0·93	0·77	0·93

Table A1. Continued

							$V_{R,calc}/V_{u,test}$				
Specimen	d: mm	ρ	f_c: MPa	d_g: mm	f_y: MPa	$V_{u,test}$: kN	Equation 13	Equation 14	Eurocode 2	ACI 318-14	MC2010 (LoA2)
Guidotti (2010)											
PG19	206	0·0076	46·2	16	510	860	0·91	0·87	0·98	1·00	0·98
PG20	201	0·0160	51·7	16	551	1094	0·96	0·90	0·97	1·24	0·96
PG23	199	0·0081	41·0	32	510	839	0·95	0·92	1·03	1·09	0·94
PG24	194	0·0162	39·8	32	551	1102	1·10	1·03	1·12	1·50	1·12
Krueger (1999)											
P0A	121	0·0100	34·6	16	480	423	1·01	1·05	0·96	1·07	1·11
Sagaseta *et al*. (2011)											
PT22	196	0·0082	67·0	16	552	989	1·03	1·02	1·05	1·02	1·10
PT31	212	0·0148	66·3	16	540	1433	1·12	1·08	1·19	1·33	1·15
Birkle and Digler (2008)											
1	124	0·0154	41·6	14	488	483	1·01	1·03	1·02	1·22	0·95
7	190	0·0130	35·0	20	531	825	0·93	0·91	1·00	1·13	0·89
10	260	0·0100	31·4	20	524	1046	0·76	0·73	0·86	0·89	0·71
Caldentey *et al*. (2013)											
1	200	0·0107	37·2	20	575	974	0·94	0·96	1·01	0·93	0·75
2	200	0·0107	37·6	20	575	956	0·92	0·94	0·99	0·91	0·72
Swamy and Ali (1982)											
S1	100	0·0060	40·1	10	462	198	0·83	0·85	0·85	0·95	0·95
S7	100	0·0070	37·4	10	462	222	0·92	0·93	0·93	1·10	1·08
Wörle (2014)											
P1	155	0·0224	37·2	16	558	612	0·92	0·86	0·91	1·76	1·08
Moreno and Sarment (2013)											
AC0	155	0·0117	56·1	16	550	685	1·00	0·99	0·97	1·10	0·89
Beutel (2002)											
P1	190	0·0081	21·9	16	572	615	0·79	0·76	0·85	0·89	0·70
Broms (1990)											
1	150	0·0091	23·4	16	681	435	0·91	0·90	1·01	1·44	1·02
Schaefers (1984)											
0	113	0·00800	21·9	32	420	280	1·06	1·01	1·22	2·00	1·43
3	170	0·00600	22·1	32	450	460	0·91	0·88	1·10	1·50	1·04
Heinzmann *et al*. (2012)											
SP1	294	0·01204	35·5	32	577	1710	0·91	0·85	1·02	1·36	0·79
Pralong (1982)											
P2	143	0·01500	35·4	16	558	628	1·05	1·04	1·09	1·61	1·23
P5	171	0·01200	27·1	16	515	626	0·90	0·87	0·99	1·44	1·04
Ladner (1998) and Ladner *et al*. (1977)											
1	240	0·01400	36·7	16	528	1095	0·85	0·80	0·90	1·34	0·90
DA6	80	0·01800	29·6	16	550	183	1·01	0·95	0·93	1·77	1·14
DA7	80	0·01800	33·1	16	550	288	1·27	1·27	1·10	1·69	1·19
DA10	80	0·01800	31·6	16	550	281	1·18	1·20	1·00	1·48	1·02
DA11	80	0·01800	30·0	16	550	324	1·24	1·28	1·01	1·40	1·02
P1	240	0·01300	27·6	32	544	1662	1·23	1·19	1·33	1·72	1·27
M1	109	0·01200	31·4	32	541	362	1·11	1·11	1·12	1·71	1·07
Bompa and Oneț (2011) and Gosav *et al*. (2013)											
DB5	155	0·00500	35·1	16	465	495	0·85	0·81	1·02	0·90	0·86
AG1	157	0·01370	17·5	16	583	570	1·03	0·98	1·04	1·44	1·08
AG2	187	0·01260	19·2	16	583	872	1·23	1·16	1·24	1·66	1·31
AG3	217	0·01200	19·8	16	583	778	0·89	0·83	0·90	1·18	0·81

Table A1. Continued

Specimen	d: mm	ρ	f_c: MPa	d_g: mm	f_y: MPa	$V_{u,test}$: kN	$V_{R,calc}/V_{u,test}$				
							Equation 13	Equation 14	Eurocode 2	ACI 318-14	MC2010 (LoA2)
Inacio *et al*. (2013)											
NS	105	0·01000	35·9	13·9	523	289	0·98	1·01	0·92	1·14	0·90
HS1	104	0·00940	126	13·9	493	413	1·08	1·11	0·89	0·88	0·87
HS2	102	0·01240	130	13·9	523	429	1·05	1·07	0·86	0·93	0·81
HS3	102	0·01480	130	13·9	523	461	1·06	1·07	0·87	1·00	0·82
Ramadane (1996)											
3	98	0·00600	26·5	10	550	169	0·80	0·81	0·92	1·30	1·01
12	98	0·01300	59·6	10	550	319	0·99	0·96	1·03	1·64	1·18
13	98	0·01300	43·1	10	550	297	0·99	0·94	1·06	1·80	1·27
14	98	0·01300	60·0	10	550	341	1·08	1·05	1·09	1·75	1·30
16	98	0·01300	97·2	10	550	362	1·01	0·98	0·99	1·46	1·10
21	98	0·01300	41·4	20	650	286	1·01	0·99	1·04	1·76	1·12
22	98	0·01300	83·2	20	650	405	1·23	1·23	1·17	1·76	1·24
23	100	0·00900	55·7	20	650	341	1·21	1·21	1·23	1·76	1·34
25	100	0·01200	32·5	10	650	244	0·91	0·89	0·96	1·65	1·09
26	100	0·01200	37·1	20	650	294	1·06	1·04	1·10	1·86	1·21
27	102	0·01000	33·3	20	650	227	0·86	0·84	0·91	1·48	0·92
Mongi (1990)											
A1	78	0·01470	21·0	20	480	176	1·19	1·16	1·19	2·67	1·53
B1	78	0·01470	29·8	20	480	160·6	0·98	0·96	0·96	2·04	1·14
B2	78	0·01470	29·8	20	480	150·4	0·92	0·90	0·90	1·91	1·06
C1	78	0·01470	29·6	20	480	200	1·10	1·13	1·07	1·99	1·16
C2	78	0·01470	29·6	20	480	221·2	1·22	1·25	1·19	2·21	1·32
C3	78	0·01470	29·6	20	480	211·5	1·17	1·19	1·13	2·11	1·24
C4	78	0·01470	29·6	20	480	185·1	1·02	1·04	0·99	1·85	1·06
C5	78	0·01470	33·4	20	480	163·5	0·87	0·89	0·84	1·53	0·86
C6	78	0·01470	33·4	20	480	227·5	1·21	1·24	1·17	2·14	1·28
C7	78	0·01470	29·6	20	480	133·4	0·74	0·75	0·72	1·33	0·73
C8	78	0·01470	30·6	20	480	167	0·91	0·93	0·89	1·64	0·92
C9	78	0·01470	30·6	20	380	200·4	1·11	1·15	1·06	1·96	1·16
C10	78	0·02940	33·4	20	380	220·8	0·92	0·92	0·90	2·07	1·14
C11	78	0·01470	29·6	20	480	170	0·94	0·96	0·91	1·69	0·96
C12	78	0·01470	29·6	20	480	160	0·88	0·90	0·86	1·60	0·89
C13	78	0·01470	29·6	20	480	190	1·05	1·07	1·02	1·89	1·09
Urban *et al*. (2013)											
II-P25	218	0·00400	32·5	16	544	920	1·12	1·08	1·51	1·71	1·53
II-P30	268	0·00400	32·5	16	544	1280	1·10	1·03	1·52	1·73	1·46
II-P35	318	0·00400	32·5	16	580	2000	1·29	1·17	1·79	2·05	1·84
Oliveira *et al*. (2004)											
L1b	108	0·01080	59·0	16	479	322·4	1·02	0·99	0·96	1·29	1·08
L1c	107	0·01090	59·0	16	479	318	1·02	0·99	0·95	1·29	1·08
L2b	106	0·01100	58·0	16	479	361	1·09	1·10	0·97	1·18	1·04
L2c	107	0·01090	57·0	16	479	330·8	0·99	1·00	0·89	1·08	0·90
L3b	107	0·01090	60·0	16	479	400	1·13	1·17	0·94	1·05	0·97
L3c	106	0·01100	54·0	16	479	357·6	1·05	1·08	0·88	1·01	0·87
L4b	106	0·01100	54·0	16	479	395	1·11	1·17	0·88	0·95	0·86
L4c	107	0·01090	56·0	16	479	404	1·11	1·17	0·88	0·94	0·86
L5b	108	0·01080	67·0	16	479	426·4	1·08	1·14	0·80	0·78	0·73
L5c	109	0·01070	63·0	16	479	446·4	1·13	1·20	0·85	0·83	0·80
Al-Yousif and Regan (2003)											
2	80	0·00982	29·0	10	472	209	1·12	1·22	0·83	0·97	0·86
4	80	0·00982	27·5	10	472	242	1·21	1·34	0·98	1·15	1·13

Table A1. Continued

							$V_{R,calc}/V_{u,test}$				
Specimen	d: mm	ρ	f_c: MPa	d_g: mm	f_y: MPa	$V_{u,test}$: kN	Equation 13	Equation 14	Eurocode 2	ACI 318-14	MC2010 (LoA2)
Ghannoum (1998)											
S1-U	110	0·00960	37·2	20	445	301	0·93	0·98	0·86	1·01	0·85
S1-B	110	0·01920	37·2	20	445	317	0·79	0·80	0·72	1·07	0·71
S2-U	110	0·00960	57·1	20	445	363	1·01	1·06	0·90	0·99	0·91
S2-B	110	0·01920	57·1	20	445	447	0·98	1·00	0·88	1·22	0·89
SE-B	110	0·01920	67·1	10	445	485	1·02	1·04	0·90	1·22	1·02
McHarg (1997)											
NSCU	110	0·00960	30·0	20	434	306	1·00	1·05	0·94	1·15	0·98
NSCB	110	0·01920	30·0	20	434	349	0·93	0·93	0·85	1·31	0·91
Kevin (2000)											
P100	100	0·00980	39·4	20	488	330	1·18	1·23	1·09	1·33	0·91
P150	150	0·00900	39·4	20	465	583	1·11	1·10	1·14	1·34	0·95
P200	200	0·00830	39·4	20	465	904	1·09	1·04	1·19	1·36	1·02
P300	300	0·00760	39·4	20	468	1381	0·86	0·77	0·99	1·11	0·83
Base (fib, 2001)											
A1/M1	114	0·01100	15·5	16	255	322	1·10	1·10	1·17	1·71	1·36
A1/M2	117	0·01500	14·7	16	282	346	1·08	1·05	1·11	1·83	1·30
A1/M3	121	0·01900	13·5	16	282	307	0·86	0·81	0·90	1·61	1·04
A1/M4	124	0·01000	13·3	16	432	259	0·82	0·77	0·91	1·33	0·91
A1/M5	117	0·01200	20·0	16	432	346	1·07	1·04	1·08	1·57	1·14
A2/M1	124	0·01000	33·6	16	255	409	1·08	1·11	1·06	1·32	1·10
A2/M2	117	0·01500	31·2	16	282	419	1·11	1·12	1·05	1·52	1·12
A2/M3	121	0·01900	30·9	16	282	430	1·00	0·99	0·95	1·49	1·01
A2/T1	124	0·01000	37·3	16	432	419	1·06	1·07	1·04	1·28	1·01
A2/T2	124	0·01700	39·3	16	432	439	0·94	0·93	0·90	1·31	0·87
A3/M1	124	0·01000	17·9	16	255	247	0·74	0·75	0·79	1·09	0·75
A3/M2	102	0·01700	18·3	16	282	336	1·19	1·18	1·16	1·91	1·41
A3/M3	117	0·01900	25·9	16	282	298	0·77	0·76	0·73	1·18	0·74
A3/T1	121	0·01000	19·6	16	432	328	1·00	0·98	1·05	1·43	1·06
A3/T2	119	0·01200	15·2	16	432	298	0·95	0·90	1·00	1·51	1·05
A4/M1	114	0·01100	36·4	16	255	259	0·76	0·78	0·71	0·90	0·63
A4/M2	119	0·01500	27·7	16	282	341	0·90	0·91	0·87	1·28	0·87
A4/M3	117	0·01900	30·6	16	322	541	1·32	1·31	1·26	1·98	1·47
A4/T1	114	0·01100	31·2	16	432	384	1·13	1·15	1·10	1·44	1·13
A4/T2	117	0·01200	27·8	16	432	402	1·14	1·14	1·13	1·54	1·17
Hegger *et al*. (2009)											
DF11	395	0·00870	21·4	16	552	2813	1·37	1·14	1·51	1·96	1·40
DF12	395	0·00870	21·1	16	552	2208	1·07	0·89	1·19	1·55	1·07
DF13	395	0·00870	21·2	16	552	1839	0·91	0·75	0·99	1·29	0·89
DF20	395	0·00870	35·7	16	552	3037	1·24	1·06	1·38	1·64	1·18
DF21	395	0·00870	36·3	16	552	2860	1·16	0·99	1·29	1·53	1·12
DF22	395	0·00870	36·4	16	552	2405	0·98	0·84	1·08	1·28	0·94
						Average	1·02	1·00	1·02	1·44	1·08
						CoV	0·13	0·14	0·15	0·25	0·21

Table A1. Continued

REFERENCES

ACI (American Concrete Institute) (2014) *ACI 318-14: Building code requirements for structural concrete and commentary*. ACI, Farmington Hills, MI, USA.

Al-Yousif AT and Regan PE (2003) Punching resistances of RC slabs supported by large and/or elongated columns. *The Structural Engineer* **81(5)**: 30–34.

Bazant ZP and Cao Z (1987) Size effect in punching shear failure of slabs. *ACI Structural Journal* **84(1)**: 44–53, http://dx.doi.org/10.14359/2785.

Bernaert M and Puech M (1966) *Compte Rendu des Travaux du Groupe de Travail Poinconnement*. Lausanne, Switzerland, Comité Européen du Béton, CEB bulletin 57.

Beutel R (2002) *Durchstanzen Schubwehrter Flachdecken im Beriech von Innenstutzen*. PhD dissertation, RWTH Aachen, Aachen, Germany.

Birkle G and Digler WH (2008) Influence of slab thickness on punching shear strength. *ACI Structural Journal* **105(2)**: 180–188, http://dx.doi.org/10.14359/19733.

Bompa DV and Oneț T (2011) Failure analysis of symmetric flat slab column connections. *Proceedings of fib Symposium, Prague, Czech Republic*.

Broms CE (1990) Punching of flat plates – a question of concrete properties in biaxial compression and size effect. *ACI Structural Journal* **87(3)**: 292–304, http://dx.doi.org/10.14359/2624.

Caldentey AP, Lavaselli PP, Peiretti HC and Fernandez FA (2013) Influence of stirrup detailing on punching shear strength of flat slabs. *Engineering Structures* **49(??)**: 855–865, http://dx.doi.org/10.1016/j.engstruct.2012.12.032.

CEN (European Committee for Standardization) (2004) EN 1992-1-1, Eurocode 2: Design of concrete structures, Part 1–1: General rules for buildings. CEN, Brussels, Belgium.

Chana PS (1987) Investigation of the mechanism of shear failure of reinforced concrete beams. *Magazine of Concrete Research* **56(6)**: 386–404, http://dx.doi.org/10.1680/macr.1987.39.141.196.

Dei Poli S, Gambarova PG and Karakoc C (1987) Aggregate interlock role in RC thin-webbed beams in shear. *ASCE Journal of Structural Engineering* **113(1)**: 1–19, http://dx.doi.org/10.1061/(ASCE)0733-9445(1987)113:1(1)).

Dei Poli S, Di Prisco M and Gambarova P (1992) Shear response, deformations, and subgrade stiffness of a dowel bar embedded in concrete. *ACI Structural Journal* **89(6)**: 665–675, http://dx.doi.org/10.14359/9645.

DSS (Dassault Systèmes Simulia Corp.) (2010) *Abaqus Analysis Users' Manual, Version 6.10*. DSS, Providence, RI, USA.

Elstner RC and Hognestad E (1956) Shearing strength of reinforced concrete slabs. *ACI Journal* **53(7)**: 29–58, http://dx.doi.org/10.14359/11501.

fib (Federation Internationale du Beton) (2001) *Punching of Structural Concrete Slabs*. fib, Lausanne, Switzerland, fib bulletin 12.

fib (2012) *Model Code 2010*. fib, Lausanne, Switzerland, fib bulletins 65 and 66.

Ghannoum CM (1998) *Effect of High-Strength Concrete on the Performance of Slab–Column Specimens*. MSc dissertation, McGill University, Montréal, Canada.

Gosav AV, Bompa DV and Kiss Z (2013) Failure analysis of interior flat-slab column connections with DHSR shear reinforcement. *Proceedings of fib Symposium, Tel-Aviv, Israel*.

Guandalini S, Burdet O and Muttoni A (2009) Punching tests of slabs with low reinforcement ratios. *ACI Structural Journal* **106(1)**: 87–95, http://dx.doi.org/10.14359/56287.

Guidotti R (2010) *Essais de Poinconnement de Dalles en Beton Arme avec Colonnes Continues Fortement Sollicitees*. PhD dissertation, Ibeton–EPFL, Lausanne, Switzerland.

Hallgren M (1996) *Punching Shear Capacity of Reinforced High-Strength Slabs*. PhD thesis, KTH Stockholm, Stockholm, Sweden, TRIT-BKN, Bulletin 23.

Hegger J, Ricker M and Sherif AG (2009) Punching strength of reinforced concrete footings. *ACI Structural Journal* **106(5)**: 706–719, http://dx.doi.org/10.14359/51663111.

Heinzmann D, Etter S, Villiger S and Jaeger T (2012) Punching tests on reinforced concrete slabs with and without shear reinforcement. *ACI Structural Journal* **109(6)**: 787–794, http://dx.doi.org/10.14359/51684122.

Inacio M, Ramos A, Lucio V and Faria D (2013) Punching of high strength concrete flat slabs. *Proceedings of fib Symposium, Tel-Aviv, Israel*.

Ince R, Yalcin E and Arslan A (2007) Size-dependent response of dowel action in RC members. *Engineering Structures* **29(6)**: 955–961, http://dx.doi.org/10.1016/j.engstruct.2006.07.006.

Kevin KLL (2000) *Influence of Size on Punching Shear Strength of Concrete Slabs*. MSc dissertation, McGill University, Montréal, Canada.

Kinnunen S and Nylander H (1960) Punching of concrete slabs without shear reinforcement. *Transactions of the Royal Institute of Technology* **158(3)**: 1–112.

Krueger G (1999) *Resistance au Poinconnement Excentre des Plancers Dalles*. PhD dissertation, EPFL, Lausanne, Switzerland, No. 2064.

Ladner M (1998) *Durchstanzversuch an Flachdeckenausshinitt*. Hochschule Luzern Technik & Architektur, Horw, Switzerland, Auftragsnummer 419–1.

Ladner M, Schaeidt W and Gus S (1977) *Experimentelle Untersuchungen an Stahlbeton-Flachdecken*. Eidgenössische Materiprüfungs- und Versuchsanstalt, Dübendorf, Switzerland, Bericht 205.

Marzouk H and Hussein H (1991) Punching shear analysis of reinforced high-strength concrete slabs. *Canadian Journal of Civil Engineers* **18(6)**: 954–963, http://dx.doi.org/10.1139/l91-118.

McHarg PJ (1997) *Effect of Fibre-Reinforced Concrete on the Performance of Slab–Column Specimens*. MSc dissertation, McGill University, Montréal, Canada.

Menetrey P (2002) Synthesis of punching failure in reinforced concrete. *Cement & Concrete Composites* **24(6)**: 497–507, http://dx.doi.org/10.1016/S0958-9465(01)00066-X.

Moe J (1961) *Shearing Strength of Reinforced Concrete Slabs and Footings Under Concentrated Loads*. Portland Cement Association, Skokie, IL, ISA, Bulletin D47.

Mongi G (1990) *A Critical Review of The Symmetric Punching Shear of Reinforced Concrete Flat Slabs*. MASc dissertation, University of Ottawa, Ottawa, Canada.

Moreno CL and Sarment AM (2013) Punching shear analysis of slab–column connections. *Engineering Computations: International Journal for Computer-Aided Engineering and Software* **30(6)**: 802–814, http://dx.doi.org/10.1108/EC-Jun-2012-0122.

Muttoni A (2008) Punching shear strength of reinforced concrete slabs without transverse reinforcement. *ACI Structural Journal* **105(4)**: 440–450, http://dx.doi.org/10.14359/19858.

Muttoni A and Fernandez Ruiz M (2012) The levels-of-approximation approach in MC2010: application to punching shear provisions. *Structural Concrete* **13(1)**: 32–41, http://dx.doi.org/10.1002/suco.201100032.

Nielsen MP (1999) *Limit Analysis and Concrete Plasticity*, 2nd edn). CRC Press, Boca Raton, FL, USA, pp. 22–31.

Oliveira DRC, Regan PE and Melo GSSA (2004) Punching resistance of RC slabs with rectangular columns. *Magazine of Concrete Research* **56(3)**: 123–138, http://dx.doi.org/10.1680/macr.2004.56.3.123.

Ottosen NS (1980) *Nonlinear Finite Element Analysis of Concrete Structures*. Risø National Laboratory, Roskilde, Denmark.

Paulay T and Loeber PJ (1974) *Shear Transfer By Aggregate Interlock*. ACI, Farmington Hills, MI, USA, ACI Special Publication 42, pp. 1–16, http://dx.doi.org/10.14359/17277.

Pralong J (1982) *Poinçonnement Symétrique des Planchers-dalles*. PhD dissertation, IBK, ETHZ, Zurich, Switzerland, http://dx.doi.org/10.3929/ethz-a-000262972.

Ramadane KE (1996) Punching shear of high performance concrete slabs. *Proceedings of the Fourth Symposium on the Utilisation of High Strength/High Performance Concrete*. Laboratoire Central des Ponts et Chaussées, Paris, France, Vol. **3**, pp. 1015–1026.

Regan PE (1986) Symmetric punching of reinforced concrete slabs. *Magazine of Concrete Research* **38(136)**: 115–128, http://dx.doi.org/10.1680/macr.1986.38.136.115.

Regan PE and Braestrup MW (1985) *Punching Shear in Reinforced Concrete*. Comité Européen du Béton, CEB Lausanne, Switzerland, Bulletin D'Information 168.

Rizk E, Marzouk H and Hussein A (2011) Punching shear of thick plates with and without shear reinforcement. *ACI Structural Journal* **108(5)**: 581–591, http://dx.doi.org/10.14359/51683215.

Sagaseta J, Muttoni A, Fernandez Ruiz M and Tassinari L (2011) Non-axis-symmetrical punching shear around internal columns of RC slabs without transverse reinforcement. *Magazine of Concrete Research* **63(6)**: 441–457, http://dx.doi.org/10.1680/macr.10.00098.

Schaefers U (1984) *Konstruction, Bemsessung und Sicherheit gegen Durchstanzen von balekenlosen Stahlbetondecken im bereich der Innenstutezen, DafStb heft 357*. Beuth-Verlag, Berlin, Germany.

Swamy R and Ali S (1982) Punching shear behaviour of reinforced slab–column connections made with steel fibre concrete. *ACI Journal* **79(5)**: 392–406, http://dx.doi.org/10.14359/10917.

Taylor HPJ (1970) *Further Tests to Determine Shear Stresses in Reinforced Concrete Beams*. Cement and Concrete Association, London, UK, Technical report TRA 438.

Tomaszewicz A (1993) *High Strength Concrete, SP2 – Plates and Shells, Report 2·3 Punching Shear Capacity of Reinforced Concrete Slabs*. SINTEF Structures and Concrete, Trondheim, Norway, Report STF70 A93082.

Urban T, Gołdyn M, Krakowski J and Krawczyk Ł (2013) Experimental investigation of punching behaviour of thick reinforced concrete slabs. *Archives of Civil Engineering* **LIX(2)**: 157–174, http://dx.doi.org/10.2478/ace-2013-0008.

Walraven JC and Reinhardt HW (1981) Theory and experiments on the mechanical behaviour of cracks in plain and reinforced concrete subjected to shear loading. *Heron* **26(1a)**: 5–68.

Wörle P (2014) Enhanced shear punching capacity by the use of post installed concrete screws. *Engineering Structures* **60(1)**: 41–51, http://dx.doi.org/10.1016/j.engstruct.2013.12.015.

WHAT DO YOU THINK?

To discuss this paper, please submit up to 500 words to the editor at journals@ice.org.uk. Your contribution will be forwarded to the author(s) for a reply and, if considered appropriate by the editorial panel, will be published as a discussion in a future issue of the journal.